

April 22, 2013

LA-UR-13-22745

arXiv:XXXXXXX

A Mesonic Analog of the Deuteron

Richard R. Silbar*

*Theoretical Division, MS-B283,
Los Alamos National Laboratory,
Los Alamos, NM 87545*

T. Goldman†

*Theoretical Division, MS-B283,
Los Alamos National Laboratory,
Los Alamos, NM 87545*

and

*Dept. of Physics and Astronomy,
University of New Mexico,
Albuquerque, NM 87501*

Abstract

Using the LAMP model for nuclear quark structure, we calculate the binding energy and quark structure of a B meson with a D meson. The larger-than-nucleon masses of the two heavy quarks and the complete absence of quark Pauli Exclusion Principle repulsive effects produce a bound state with structure ranging from a deuteron-like state to a fully mixed four-quark state. Unlike the deuteron, however, pion exchange does not provide the dominant contribution to binding.

PACS numbers: 12.39.Ki, 12.39.Mk, 12.39.Pn, 12.38.Lg, 24.85.+p, 21.45.+v

* silbar@lanl.gov

† tgoldman@lanl.gov

I. INTRODUCTION

The relativistic Los Alamos Model Potential [1, 2] (LAMP) has been used to describe the binding and structure of ^3He and ^4He , including a good description [3] of the deep inelastic structure function of ^3He . It does not, however, describe the deuteron due to the large separation of the nucleons and the dominance of single-pion exchange contributions there. The LAMP, lacking quark-exchange correlations, best encompasses medium and short-range meson exchanges (two-pion, ρ , and the like). It must therefore be supplemented with long-range single-pion-exchange contributions [4] for a better description of nuclear binding energies.

In this paper, however, because the isodoublet B and D mesons are much more massive than nucleons, the localization energy is much reduced. This brings them into closer proximity than the nucleons in a deuteron, or indeed, even in a large nucleus. Furthermore, the quark content does not require any pairs of quarks with the same (internal) quantum numbers, obviating the contribution of any of the (quark) Pauli exclusion effects that contribute to the short range repulsion between nucleons. Thus, this is a system in which one can expect greater accuracy of the LAMP and a significantly more deeply bound state than the deuteron.

When this B - D bound state is observed, the deviation from our predictions here will provide a very good measure of the center of mass motion and breathing mode collective excitations. These are difficult to remove in the LAMP due to its relativistic nature. Since the non-relativistic analog model, the Quark Delocalization and Color Screening Model of Wang *et al.* [5] gives very similar results to the LAMP after removing such effects, we expect them to be small and hence, that our predictions here are reasonably accurate.

A. Initial Concepts

The LAMP treats the confining potential for quarks (and antiquarks) as a fixed scalar interaction in a Born-Oppenheimer-like picture, with the location of the potential minimum defining the system location. Quarks bound in a baryon or meson are treated as being bound within this potential rather than directly to each other. As such, there are immediate concerns about removing center-of-mass and breathing mode contributions to the evaluated

state energy. This concern is ameliorated by comparing the energy of the interacting system of the two heavy mesons with the value at large (essentially infinite) separation.

In this paper, in addition to the confining Lorentz scalar potential of the LAMP, we have included a Lorentz vector potential, as is required from the observed small spin-orbit interaction in the non-relativistic quark model.[6] In fact, the vector potential is also taken as linear, attractive, but without a Coulomb-like contribution, as discussed in Ref. [7].

In the LAMP, the confining potentials for each hadron are distributed in an array and are truncated on the mid-planes between them. While complex in general, for the case of interest here – two heavy mesons – the structure is very similar to that of the hydrogen molecule in the Born-Oppenheimer approximation, except for the linear vs. inverse distance form of the potential. In this case, the large masses of the c and b quarks further enhance the credibility of the approximation – they may be taken in the conventional heavy quark limit [8] as the fixed origins of the confining potentials for the light anti-quarks that complete each meson.

At large separation between the heavy quarks, confinement guarantees the isolation of the light quark wave functions from each other. However, as the two mesons approach within a distance less than a few times their root-mean-square radii, the truncation of the confining potential allows for tunneling of each light anti-quark wave function into the confinement region of the other heavy quark rather than the one to which it is bound. The concept behind this is that a quark can only be confined to nearest center of color attraction, as in string-flip models [9], for example. This spreading out, or delocalization, of the wave functions naturally reduces the localization energy and provides an initial source of binding between the two hadrons.

B. Color magnetic and quantum number issues

In nuclei and other systems, this basic consideration is complicated by additional elements: there are color-6 combinations of quarks and color-magnetic spin interactions of significance on the scale of the binding energy. Here again, the concerns raised by these considerations are considerably reduced – the color magnetic interactions between the heavy quarks are reduced to negligible values by their large masses. The light quark color magnetic interactions with the heavy quarks are also significantly reduced. Only the light-quark

to light-quark color magnetic interaction remains. This is at most ≈ 50 MeV as seen [10] in individual hadrons (nucleons, Δ 's, light spin-0, and spin-1 mesons) where it depends on the color and spin-strong-isospin combinations determined by the constraints of statistics. Furthermore, here the presence of both color **6** and color **3** combinations, as well as spin-1 and spin-0 elements, make it clear that strong cancellations of these color magnetic effects to low levels are to be expected. Therefore, in this paper we will only estimate these (in Sec. XI), ignoring details. We also will neglect the very small electro-magnetic contributions.

Because of these simplifications, we will mostly ignore the fact that there are two neutral states ($B^- D^+$ and $\bar{B}^0 D^0$) that should exist and mix, splitting to form states of definite strong isospin (0 and 1) although both have $I_3 = 0$. They also allow us to ignore the detailed spin structures, ranging from $J = 0$ to $J = 2$, the latter with all of the quark spins aligned. Also unlike the individual nucleon case, the c and b quarks may combine anti-symmetrically to form a color $\bar{\mathbf{3}}$ state or symmetrically to form a color **6**. In the first case, the light anti-quarks must form a color **3** antisymmetrically, thus requiring the spin-isospin combination to be symmetric ($I=0, J=0$, or $I=1, J=1$) and in the latter, the opposite is true – a color $\bar{\mathbf{6}}$ and ($I=1, J=0$, or $I=0, J=1$).

Again, these allowed spin-isospin combinations for the light quarks would only produce significant energy differences if the color magnetic interaction were larger. The color **6** combination of the heavy quarks would not be expected to produce any attraction, as indeed no such components appear in baryons, but the color $\bar{\mathbf{3}}$ combination would. Neither of these effects is included here as the channel to color neutralization by decomposition into two color-singlet mesons (B and D) is almost open. In any event, symmetrization and antisymmetrization between the c and b quarks is moot as they are eminently quantum mechanically distinguishable.

We turn now to the detailed calculations of the light (anti)quark wave functions in the double well defined by the Born-Oppenheimer-fixed heavy quarks.

II. THE TWO-WELL WAVE FUNCTION

For two wells separated by $\pm \delta$ at dimensionless [11] positions $\mathbf{w}_{\pm} = \{0, 0, \pm \delta\}$ along the z -axis (see Fig. 1), we define the wave function

$$\Psi_L(\mathbf{r}) = \psi(\mathbf{r}_-) + \epsilon \psi(\mathbf{r}_+), \quad \text{where} \quad \mathbf{r}_{\pm} = \mathbf{r} + \mathbf{w}_{\pm} = \{x, y, z \pm \delta\}. \quad (1)$$

This represents, for example, a light \bar{u} -quark (i.e., which we assume to be massless) mostly moving and confined in the well at r_- (the “left”) provided by a heavy b -quark. There may be some “leakage,” represented by ϵ , into the “right” well at r_+ , provided by, say, a heavy c -quark. We assume that the b and c quark masses are large enough to justify a Born-Oppenheimer approximation of this sort. There is a similar wave function Ψ_R with r_- and r_+ interchanged in Eq. (1) for a light \bar{d} -quark mostly confined to the well at r_+ with ϵ -leakage into the well at r_- . We wish to determine what the best values of the parameters δ and ϵ are that provide a four-quark or molecular-like binding that form a $b\bar{u}c\bar{d}$ system. The b and c are well separated compared with their Compton sizes. Since they have little, if any, wave function overlap and have distinct quantum numbers, anti-symmetrization issues are irrelevant. For the rest of the paper we will drop the subscript L on Ψ , but it should be borne in mind when we finally compose the $b\bar{u}c\bar{d}$ four-quark state.

We take the ψ 's in Eq. (1) to be dimensionless four-component Dirac wave functions for light (here, assumed massless) u - and d -quarks. They are solutions of

$$H_D \psi = [-i\boldsymbol{\alpha} \cdot \nabla + V(\mathbf{r}) + \beta S(\mathbf{r})] \psi = E \psi . \quad (2)$$

Here $V(\mathbf{r})$ is the time component of a Lorentz four-vector and $S(\mathbf{r})$ is a Lorentz scalar potential (both to be specified below). With the Pauli spinor χ assumed to be quantized along the z -direction with spin-projection m_s , the normalized four-component s -wave Dirac wave function $\psi(\mathbf{r})$ is

$$\psi_{m_s}(\mathbf{r}) = \frac{1}{\sqrt{4\pi}} \begin{pmatrix} \psi_a(r) \chi_{m_s} \\ i\boldsymbol{\sigma} \cdot \mathbf{r} \psi_b(r) \chi_{m_s} \end{pmatrix} . \quad (3)$$

The upper and lower radial wave functions $\psi_a(r)$ and $\psi_b(r)$ can be chosen real. We have calculated them by solving the coupled radial Dirac equations [12] for (dimensionless) linear Lorentz vector and scalar potentials of the form [11]

$$V(r) = r - R \quad \text{and} \quad S(r) = r . \quad (4)$$

Here $-R$ is a negative displacement pushing the vector potential $V(r)$ down below the scalar potential $S(r)$, so that confinement trumps Klein-Gordon pair creation.[6]

The solid curves in Fig. 2 show the calculated (dimensionless [11]) $1S$ wave functions $\psi_a(r)$ and $r\psi_b(r)$ when the potentials have $R = 1.92$, $\kappa^2 = 1.253$ GeV/fm. Physical dimensions are obtained by dividing the dimensionless r , R , etc., by $\kappa = 2.52$ fm $^{-1}$. The ground

state eigenenergy resulting from this calculation is 0.375 GeV. These potentials provide a reasonable fit to the $c\bar{c}$ spectrum.[7]

For the calculations presented below, the $\psi_{a,b}$ have both been fitted to sums of Gaussians,

$$\psi_a(r) = \sum_i a_i e^{-\mu_i r^2/2}, \quad \psi_b(r) = \sum_i b_i e^{-\mu_i r^2/2}, \quad (5)$$

where the a_i , b_i , and μ_i are dimensionless numbers. We found it necessary to go to six terms, so that evaluating the upper and lower components of the left-hand-side of Eq. (2) gives reasonable agreement with the right-hand-side. The fitted parameters are

$$\begin{aligned} \mu_i &= \{ 1.0, 1.3, 1.6, 2.0, 4.0, 8.0 \} \\ a_i &= \{ 0.492649, -0.687482, 1.84609, -0.00246039, 0.258295, 0.0956581 \} \\ b_i &= \{ -0.0571296, 1.03367, -1.18398, 1.33989, 0.162575, 0.299479 \}. \end{aligned} \quad (6)$$

The fitted $\psi_a(r)$ and $r\psi_b(r)$ are shown as the dashed curves in Fig. 2, largely overlying the solid curves from the solution of the Dirac equation. To check the quality of the fits we have evaluated the single-quark expectation value of the Hamiltonian, $\langle H_D \rangle = 0.7545$, which is slightly larger than the (dimensionless) energy eigenvalue $E = 0.7540$ (which, for a variational trial function, is as it should be).

III. EXPANDING $\langle H_D^2 \rangle$

The idea is that we will want to minimize the expectation value $\langle H_D^2 \rangle^{1/2}$ (and the color-magnetic interaction between the quarks) with respect to the parameters ϵ and δ to bound (approximately) the energy for the four-quark system consisting of b , c , \bar{u} , and \bar{d} . $\langle H_D^2 \rangle$ is required for a variational bound as, due to negative energy states, $\langle H_D \rangle$ itself is unbounded below. The Dirac Hamiltonian H_D is displayed in Eq. (2) but now, for the two-well case (Fig. 1), the potentials are

$$V(\mathbf{r}) = \begin{cases} r_- - R, & \text{if } z > 0 \\ r_+ - R, & \text{if } z < 0 \end{cases} \quad \text{and} \quad S(\mathbf{r}) = \begin{cases} r_-, & \text{if } z > 0 \\ r_+, & \text{if } z < 0 \end{cases}. \quad (7)$$

As already mentioned, $-R$ is a negative offset so the vector potential lies below the scalar.

The exact *two-well* energy E is in principle found by solving for the eigenvalue of

$$H_D \Psi(\mathbf{r}) = E \Psi(\mathbf{r}), \quad (8)$$

with Ψ given in Eq. (1). This being difficult, we instead chose to find an approximate value of the four-quark energy E by the above-mentioned minimization of $\langle H_D^2 \rangle^{1/2}$.

After some algebra one finds

$$H_D^2 = -\nabla^2 + V^2(\mathbf{r}) + S^2(\mathbf{r}) + 2\beta V(\mathbf{r}) S(\mathbf{r}) - i\boldsymbol{\alpha} \cdot [(\nabla V(\mathbf{r})) + \beta (\nabla S(\mathbf{r}))] - 2i V(\mathbf{r}) \boldsymbol{\alpha} \cdot \nabla . \quad (9)$$

The lack of a term like $-2i S(\mathbf{r}) \boldsymbol{\alpha} \cdot \nabla$ is because of a cancellation as the Dirac operators $\boldsymbol{\alpha}$ and β anti-commute. The first four terms of H_D^2 are “diagonal” (generically, \mathcal{O}_D) in that they connect ψ_a to ψ_a and ψ_b to ψ_b , while the last two terms are “off-diagonal” (\mathcal{O}_{OD}) connecting ψ_b to ψ_a .

As a second check on our Gaussian fits of ψ_a and ψ_b , Eqs. (5) and (6), we evaluated the expectation $\langle H_D^2 \rangle$ to be 0.5691, again slightly larger than $E^2 = 0.5685$, as it should be.

The following six sections describe how we calculate the expectation values of the terms in Eq. (9). These are basically integrals over various Gaussians, and are often messy formulas involving error functions. A reader less interested in these details may wish to skip directly to Sec. X, which presents the numerical results of these calculations.

IV. GENERAL REMARKS ON CALCULATING THE EXPECTATIONS

The reason for approximating our numerical radial wave functions ψ_a and ψ_b as sums of Gaussians is that it allows us to calculate the expectation values of each of the terms of H_D^2 analytically. Given an analytic expression for H_D^2 allows us to plot it quickly and precisely as a function of δ and ϵ . To do these integrations, we have relied heavily on programs such as Mathematica and Maple. As will be seen, the final results can sometimes be messy and often involve error functions [13] because of the Gaussians being integrated.

For the diagonal operators of H_D^2 we will calculate the upper and lower contributions separately,

$$\langle \Psi | \mathcal{O}_D | \Psi \rangle = \langle \Psi | \mathcal{O}_D | \Psi \rangle_A + \langle \Psi | \mathcal{O}_D | \Psi \rangle_B . \quad (10)$$

The B -expectations are more complicated than those for A because of the factors of $-i\boldsymbol{\sigma} \cdot \mathbf{r}_\pm$ multiplying the radial ψ_b ’s. However, for some diagonal operators, as will be seen below, the B -expectations are not always needed. In any case, from Eq. (5) we expand these diagonal

operator expectations as

$$\langle \Psi | \mathcal{O}_D | \Psi \rangle_A = \sum_{i,j} a_i a_j I_{ij} , \quad \langle \Psi | \mathcal{O}_D | \Psi \rangle_B = \sum_{i,j} b_i b_j J_{ij} , \quad (11)$$

where the I_{ij} and J_{ij} are integrals over Gaussians.

First, we separate out the quadratic dependence on ϵ as

$$I_{ij} = I_{ij}^{(0)} + \epsilon I_{ij}^{(1)} + \epsilon^2 I_{ij}^{(2)} = (1 + \epsilon^2) I_{ij}^{(0)} + \epsilon I_{ij}^{(1)} , \quad (12)$$

and likewise for the lower-component B -integrals J_{ij} . The second equality here comes about because parity symmetry ensures that the $I_{ij}^{(2)} = I_{ij}^{(0)}$, etc. We will refer to the $I_{ij}^{(0)}$ as “direct terms,” in that they connect Gaussians with $\mu_j r_-^2/2$ to those with $\mu_i r_-^2/2$ (and similarly for $I_{ij}^{(2)}$ with r_+). Recalling the $1/4\pi$ from the normalization of the ψ 's, we ensure the symmetry under the interchange of indices i and j by writing

$$I_{ij}^{(0)} = \frac{1}{8\pi} \int d^3r \left\{ e^{-\mu_i r_-^2/2} \mathcal{O}_D e^{-\mu_j r_-^2/2} + e^{-\mu_j r_-^2/2} \mathcal{O}_D e^{-\mu_i r_-^2/2} \right\} . \quad (13)$$

The direct integrals $J_{ij}^{(0)}$ have a similar form but with $\boldsymbol{\sigma} \cdot \mathbf{r}_- \mathcal{O}_D \boldsymbol{\sigma} \cdot \mathbf{r}_-$ in place of the \mathcal{O}_D .

The “cross terms” $I_{ij}^{(1)}$ are more complicated integrals than the $I_{ij}^{(0)}$, and likewise for $J_{ij}^{(1)}$. They connect Gaussians with $\mu_j r_-^2/2$ to $\mu_j r_+^2/2$ and vice versa. Thus, on symmetrizing in i and j ,

$$I_{ij}^{(1)} = \frac{1}{8\pi} \int d^3r \left\{ \left[e^{-\mu_i r_-^2/2} \mathcal{O}_D e^{-\mu_j r_+^2/2} + e^{-\mu_i r_+^2/2} \mathcal{O}_D e^{-\mu_j r_-^2/2} \right] + \left[e^{-\mu_j r_-^2/2} \mathcal{O}_D e^{-\mu_i r_+^2/2} + e^{-\mu_j r_+^2/2} \mathcal{O}_D e^{-\mu_i r_-^2/2} \right] \right\} \quad (14)$$

The $J_{ij}^{(1)}$ have a similar form but with \mathcal{O}_D replaced by $\boldsymbol{\sigma} \cdot \mathbf{r}_- \mathcal{O}_D \boldsymbol{\sigma} \cdot \mathbf{r}_+$ or $\boldsymbol{\sigma} \cdot \mathbf{r}_+ \mathcal{O}_D \boldsymbol{\sigma} \cdot \mathbf{r}_-$, as appropriate.

Each of the off-diagonal operators in Eq. (9) has the general form

$$\mathcal{O}_{OD} = -i\boldsymbol{\alpha} \cdot \mathbf{X} = \begin{bmatrix} 0 & -i\boldsymbol{\sigma} \cdot \mathbf{X}_{12} \\ -i\boldsymbol{\sigma} \cdot \mathbf{X}_{21} & 0 \end{bmatrix} \quad (15)$$

where the \mathbf{X}_{12} and \mathbf{X}_{21} are vector-operators that may not be equal because of the possible presence of the diagonal β matrix in \mathcal{O}_{OD} .

The direct terms of the off-diagonal expectation $\langle \mathcal{O}_{OD} \rangle$ involve several terms because the upper component of $\Psi^\dagger(\mathbf{r}_-)$ connects through $-i\boldsymbol{\sigma} \cdot \mathbf{X}_{12}$ to the lower component of $\Psi(\mathbf{r}_-)$ at the same time that the lower component of $\Psi^\dagger(\mathbf{r}_-)$ connects through $-i\boldsymbol{\sigma} \cdot \mathbf{X}_{21}$ to

the upper component of $\Psi(\mathbf{r}_-)$. We therefore have to keep the sums over the a 's and b 's in Eq. (5) as parts of the integrand. Again symmetrizing in i and j ,

$$\begin{aligned} \langle \mathcal{O}_{OD}^{(0)} \rangle = \frac{1}{8\pi} \sum_{i,j} \int d^3r \left\{ e^{-\mu_i r_-^2/2} [-a_i b_j (\boldsymbol{\sigma} \cdot \mathbf{X}_{12})(\boldsymbol{\sigma} \cdot \mathbf{r}_-) \right. \\ \left. + a_j b_i (\boldsymbol{\sigma} \cdot \mathbf{r}_-)(\boldsymbol{\sigma} \cdot \mathbf{X}_{21})] e^{-\mu_j r_-^2/2} \right. \\ \left. + e^{-\mu_j r_-^2/2} [-a_j b_i (\boldsymbol{\sigma} \cdot \mathbf{X}_{12})(\boldsymbol{\sigma} \cdot \mathbf{r}_-) \right. \\ \left. + a_i b_j (\boldsymbol{\sigma} \cdot \mathbf{r}_-)(\boldsymbol{\sigma} \cdot \mathbf{X}_{21})] e^{-\mu_i r_-^2/2} \right\} . \quad (16) \end{aligned}$$

The cross terms of $\langle \mathcal{O}_{OD} \rangle$ have even more terms because the $\Psi^\dagger(\mathbf{r}_+)$ connects to $\Psi(\mathbf{r}_-)$ at the same time that $\Psi^\dagger(\mathbf{r}_-)$ connects to $\Psi(\mathbf{r}_+)$. It becomes

$$\begin{aligned} \langle \mathcal{O}_{OD}^{(1)} \rangle = \frac{1}{8\pi} \sum_{i,j} \int d^3r \left\{ e^{-\mu_i r_+^2/2} [-a_i b_j (\boldsymbol{\sigma} \cdot \mathbf{X}_{12})(\boldsymbol{\sigma} \cdot \mathbf{r}_-) \right. \\ \left. + a_j b_i (\boldsymbol{\sigma} \cdot \mathbf{r}_+)(\boldsymbol{\sigma} \cdot \mathbf{X}_{21})] e^{-\mu_j r_-^2/2} \right. \\ \left. + e^{-\mu_i r_-^2/2} [-a_i b_j (\boldsymbol{\sigma} \cdot \mathbf{X}_{12})(\boldsymbol{\sigma} \cdot \mathbf{r}_+) \right. \\ \left. + a_j b_i (\boldsymbol{\sigma} \cdot \mathbf{r}_-)(\boldsymbol{\sigma} \cdot \mathbf{X}_{21})] e^{-\mu_j r_+^2/2} \right. \\ \left. + e^{-\mu_j r_+^2/2} [-a_j b_i (\boldsymbol{\sigma} \cdot \mathbf{X}_{12})(\boldsymbol{\sigma} \cdot \mathbf{r}_-) \right. \\ \left. + a_i b_j (\boldsymbol{\sigma} \cdot \mathbf{r}_+)(\boldsymbol{\sigma} \cdot \mathbf{X}_{21})] e^{-\mu_i r_-^2/2} \right. \\ \left. + e^{-\mu_j r_-^2/2} [-a_j b_i (\boldsymbol{\sigma} \cdot \mathbf{X}_{12})(\boldsymbol{\sigma} \cdot \mathbf{r}_+) \right. \\ \left. + a_i b_j (\boldsymbol{\sigma} \cdot \mathbf{r}_-)(\boldsymbol{\sigma} \cdot \mathbf{X}_{21})] e^{-\mu_i r_+^2/2} \right\} . \quad (17) \end{aligned}$$

The integrations for the I 's, J 's, and in Eqs. (16) and (17) can best be done using (dimensionless) cylindrical coordinates, $\rho = (x^2 + y^2)^{1/2}$, θ , and z . The θ integrations are trivial, providing a factor of 2π , which will cancel with the $1/4\pi$ coming from the normalizations of the ψ 's in Eq. (3) to give an overall factor of $1/2$ before each double integral over ρ and z . It usually is easier to do the ρ -integration (from 0 to $+\infty$) first. Because $V(\mathbf{r})$ and $S(\mathbf{r})$ depend on r_- when $z > 0$ and on r_+ when $z < 0$, we need to do the z -integration separately for those regions, i.e., for z from $-\infty$ to 0 and then for z from 0 to $+\infty$. The separate results are then added and simplified to give the final integral.

We will distinguish the results for the expectations of the different operators in Eq. (9) by an appropriate subscript. For example, for $O_D = \nabla^2$, we will write $I_{ij}^{(0,1)}$ as $I_{ij, <\nabla^2>}^{(0,1)}$, and similarly for the J_{ij} integrals.

V. NORMALIZING Ψ

While the Dirac ψ 's are themselves properly normalized, the two-well Ψ is not. For this we need to calculate the expectation values of $\mathcal{O}_D = 1$ to find

$$N^2(\delta, \epsilon) = \int d^3r \Psi^\dagger \Psi = \langle \Psi | 1 | \Psi \rangle = \langle \Psi | 1 | \Psi \rangle_A + \langle \Psi | 1 | \Psi \rangle_B . \quad (18)$$

We make the expansion in ϵ as in Eq. (12) above. The direct-term integrals for the expectation $\langle 1 \rangle$ are, noting that for the $J_{ij, <1>}^{(0)}$ we also have a factor of $(\boldsymbol{\sigma} \cdot \mathbf{r}_-)(\boldsymbol{\sigma} \cdot \mathbf{r}_-) = r_-^2$ in the integrand,

$$I_{ij, <1>}^{(0)} = \left[\frac{\pi}{2(\mu_i + \mu_j)^3} \right]^{1/2} \quad (19)$$

$$J_{ij, <1>}^{(0)} = 3 \left[\frac{\pi}{2(\mu_i + \mu_j)^5} \right]^{1/2} , \quad (20)$$

both independent of δ .

The cross-term integrals do depend on δ . For the $J_{ij, <1>}^{(1)}$ we need the factor [14]

$$(\boldsymbol{\sigma} \cdot \mathbf{r}_+)(\boldsymbol{\sigma} \cdot \mathbf{r}_-) = \mathbf{r}_+ \cdot \mathbf{r}_- = \rho^2 + z^2 - \delta^2 \quad (21)$$

in the integrand. Proceeding as in Sec. IV, we find

$$I_{ij, <1>}^{(1)} = \left[\frac{2\pi}{(\mu_i + \mu_j)^3} \right]^{1/2} e^{-2\mu_i \mu_j \delta^2 / (\mu_i + \mu_j)} , \quad (22)$$

$$J_{ij, <1>}^{(1)} = \left[3(\mu_i + \mu_j) - 4\mu_i \mu_j \delta^2 \right] \left[\frac{2\pi}{(\mu_i + \mu_j)^7} \right]^{1/2} e^{-2\mu_i \mu_j \delta^2 / (\mu_i + \mu_j)} . \quad (23)$$

Note that, when $\delta = 0$, $I_{ij, <1>}^{(1)} = 2 I_{ij, <1>}^{(0)}$, and $J_{ij, <1>}^{(1)} = 2 J_{ij, <1>}^{(0)}$. This is a common feature for all the expectations here and below. This is necessary so that, for example, when $\delta = 0$ and $\epsilon = 1$, one recovers a result that is four times that when $\delta = 0$ and $\epsilon = 0$.

We see from Eq. (22) that $I_{ij, <1>}^{(1)}$, as a function of δ , is a decaying Gaussian (as in Fig. 3A). On the other hand, $J_{ij, <1>}^{(1)}$ falls off from its peak at $\delta = 0$, goes through zero, and has a mild minimum before decaying to zero at large δ^2 (as in Fig. 3B).

Combining all terms,

$$N^2(\epsilon, \delta) = \sum_{i,j} a_i a_j \left[(1 + \epsilon^2) I_{<1>}^{(0)} + \epsilon I_{<1>}^{(1)} \right] + \sum_{i,j} b_i b_j \left[(1 + \epsilon^2) J_{<1>}^{(0)} + \epsilon J_{<1>}^{(1)} \right] \quad (24)$$

and the normalized Ψ is obtained by multiplying Eq. (1) by $1/N(\epsilon, \delta)$.

Figure 4 shows a plot of $N^2(\epsilon, \delta)$ for the values of the a 's, b 's, and μ 's that were fitted to the normalized ψ_a and ψ_b , Eq. (6). We have checked that, for these values, $N^2(0, 0) = 0.9858 \approx 1$ and $N^2(1, 0) = 3.9430 \approx 4$, as they should but with some deviation ($\approx 2\%$) coming from the inexactness of the fitting. The ratio of the two values is 4 to high accuracy.

To illustrate what "leakage" from one well to the other might look like, Fig. 5 shows a plot of the upper component of the normalized Ψ as a function of ρ (running from 0 to 2) and z (running from -3.5 to +3.5) for $\epsilon = 0.5$ and $\delta = 1.1$.

VI. EVALUATING THE DIAGONAL EXPECTATION $\langle -\nabla^2 \rangle$

First, note that, for $\mathbf{r}_\pm = \{x, y, z \pm \delta\}$, the i th component of the gradient

$$\nabla_i = \frac{\partial}{\partial x_i} = \nabla'_i = \frac{\partial}{\partial x'_i} \quad \text{for} \quad \mathbf{r}' = \{x' = x, y' = y, z' = z \pm \delta\} = \mathbf{r}_\pm \quad (25)$$

since each $\partial x'_i / \partial x_i = 1$. Thus we can replace the result of the Laplacian with respect to r acting on a function such as $\psi_a(r_-)$ with that for a Laplacian with respect to r_- acting on that function. For spherical coordinates, $-\nabla^2$ on the angle-independent $e^{-\mu_j r_-^2/2}$ then becomes

$$-\nabla^2 e^{-\mu_j r_-^2/2} = -\nabla'^2 e^{-\mu_j r_-^2/2} = -\frac{1}{r_-} \frac{d^2}{dr_-^2} \left(r_- e^{-\mu_j r_-^2/2} \right) = -\mu_j (\mu_j r_-^2 - 3) e^{-\mu_j r_-^2/2}, \quad (26)$$

whence the three-dimensional integral reduces, after symmetrizing and canceling factors of 4π , to

$$I_{ij, <-\nabla^2>}^{(0)} = 3 \mu_i \mu_j \left[\frac{\pi}{2(\mu_i + \mu_j)^5} \right]^{1/2}, \quad (27)$$

independent of δ .

For the B -integrals things are more complicated because of the $\boldsymbol{\sigma} \cdot \mathbf{r}_-$ factor to the right of the Laplacian. After some algebra,

$$-(\boldsymbol{\sigma} \cdot \mathbf{r}_- \nabla^2 \boldsymbol{\sigma} \cdot \mathbf{r}_-) e^{-\mu_j r_-^2/2} = -r_-^2 \mu_j (\mu_j r_-^2 - 5) e^{-\mu_j r_-^2/2} \quad (28)$$

whence

$$J_{ij, <-\nabla^2>}^{(0)} = 15 \mu_i \mu_j \left[\frac{\pi}{2(\mu_i + \mu_j)^7} \right]^{1/2}, \quad (29)$$

also independent of δ .

The cross terms, again, do depend on δ .

$$I_{ij, <-\nabla^2>}^{(1)} = \mu_i \mu_j [3(\mu_i + \mu_j) - 4\mu_i \mu_j \delta^2] \left[\frac{2\pi}{(\mu_i + \mu_j)^7} \right]^{1/2} e^{-2\mu_i \mu_j \delta^2 / (\mu_i + \mu_j)} . \quad (30)$$

A plot of this integral as a function of δ looks like Fig. 3B.

For the corresponding B -cross term, one proceeds in the same manner but, instead of Eq. (28), we need [14]

$$-(\boldsymbol{\sigma} \cdot \mathbf{r}_+ \nabla^2 \boldsymbol{\sigma} \cdot \mathbf{r}_-) e^{-\mu_j r_-^2 / 2} = -(\rho^2 + z^2 - \delta^2) \mu_j (\mu_j r_-^2 - 5) e^{-\mu_j r_-^2 / 2} . \quad (31)$$

We find

$$J_{ij, <-\nabla^2>}^{(1)} = \mu_i \mu_j [15(\mu_i + \mu_j)^2 - 40\mu_i \mu_j (\mu_i + \mu_j) \delta^2 + 16\mu_i^2 \mu_j^2 \delta^4] \times \left[\frac{2\pi}{(\mu_i + \mu_j)^{11}} \right]^{1/2} e^{-2\mu_i \mu_j \delta^2 / (\mu_i + \mu_j)} . \quad (32)$$

This integral as a function of δ also looks like Fig. 3B, but because it is quartic, it is slightly positive beyond $\delta = 1.7$.

VII. EVALUATING THE EXPECTATION OF $V^2 + S^2 + 2\beta VS$

This is also a diagonal operator. The linear vector potential $V(\mathbf{r})$ differs from the linear scalar potential $S(\mathbf{r})$ by a negative offset $-R$. In $\langle V^2(\mathbf{r}) \rangle$ the integrals of $\langle r_{\pm}^2 \rangle$ are the same as those for $\langle S^2(\mathbf{r}) \rangle$. Here, $\langle r_{\pm}^2 \rangle$ means the integration of r_-^2 when $z > 0$ and of r_+^2 when $z < 0$. Thus we (schematically) expand the diagonal $V^2 + S^2 + 2\beta VS$ as

$$\langle V^2 + S^2 + 2\beta VS \rangle = 2 \langle r_{\pm}^2 \rangle (1 + \beta) - 2R \langle r_{\pm} \rangle (1 + \beta) + R^2 \langle 1 \rangle . \quad (33)$$

The factor of $(1 + \beta)$ ensures that only the upper components of Ψ contribute to the first two expectation values. That is, we only need to calculate the A -integrals (the I 's) for those terms. The expectation value $\langle 1 \rangle$ multiplying R^2 does have contributions from the lower components and their integrals $I_{<1>}^{(0)}$, $I_{<1>}^{(1)}$, $J_{<1>}^{(0)}$, and $J_{<1>}^{(1)}$ are given in Sec. V.. The integrals for the operators $\langle r_{\pm}^2 \rangle$ and $\langle r_{\pm} \rangle$ are rather more complicated and their analytic forms are presented next.

A. $\mathcal{O}_D = r_{\pm}^2$

The direct integral for this operator is

$$I_{ij, <r_{\pm}^2>}^{(0)} = - \frac{2\delta}{(\mu_i + \mu_j)^2} e^{-(\mu_i + \mu_j) \delta^2/2} + \left[\frac{\pi}{2(\mu_i + \mu_j)^5} \right]^{1/2} \left[3 + 2(\mu_i + \mu_j) \delta^2 \operatorname{Erfc} \left(\sqrt{\frac{(\mu_i + \mu_j)}{2}} \delta \right) \right]. \quad (34)$$

Note the linear dependence on δ , which gives rise to a shallow minimum near the origin before the function returns to its initial value, as in Fig. 3C.

The cross-term integral for $<r_{\pm}^2>$ is

$$I_{ij, <r_{\pm}^2>}^{(1)} = - \frac{4\delta}{(\mu_i + \mu_j)^2} e^{-(\mu_i + \mu_j) \delta^2/2} + \left[\frac{2\pi}{(\mu_i + \mu_j)^7} \right]^{1/2} e^{-2\mu_i \mu_j \delta^2/(\mu_i + \mu_j)} \times \left\{ 3(\mu_i + \mu_j) + 2(\mu_i^2 + \mu_j^2) \delta^2 - 2(\mu_i^2 - \mu_j^2) \delta^2 \operatorname{Erf} \left(\frac{(\mu_i - \mu_j)}{\sqrt{2(\mu_i + \mu_j)}} \delta \right) \right\}, \quad (35)$$

which also has odd terms in δ . In this case, as a function of δ , $I_{ij, <r_{\pm}^2>}^{(1)}$ falls off smoothly to zero from its peak value at $\delta = 0$, as in Fig. 3D. $I_{ij, <r_{\pm}^2>}^{(1)}$ is symmetric in i and j because $\operatorname{Erf}(-x) = -\operatorname{Erf}(x)$, $I_{ij, <r_{\pm}^2>}^{(1)} = I_{ji, <r_{\pm}^2>}^{(1)}$. Also, as expected,

$$I_{<r_{\pm}^2>}^{(1)} = 2 I_{<r_{\pm}^2>}^{(0)} = 3 \left[\frac{2\pi}{(\mu_i + \mu_j)^5} \right]^{1/2} \quad (36)$$

when $\delta = 0$.

B. $\mathcal{O}_D = r_{\pm}$

The direct term for this operator is

$$\begin{aligned}
I_{ij, <r_{\pm}>}^{(0)} = & \frac{1}{2(\mu_i + \mu_j)^2} [4 + 2 e^{-2(\mu_i + \mu_j) \delta^2} - 3 e^{-(\mu_i + \mu_j) \delta^2/2}] \\
& - \frac{1}{2\delta} \left[\frac{\pi}{2(\mu_i + \mu_j)^5} \right]^{1/2} \times \\
& \left\{ (\mu_i + \mu_j) \delta^2 - (1 + 4(\mu_i + \mu_j) \delta^2) \operatorname{Erf} \left(\sqrt{2(\mu_i + \mu_j)} \delta \right) \right. \\
& \left. + (1 + 3(\mu_i + \mu_j) \delta^2) \operatorname{Erf} \left(\sqrt{(\mu_i + \mu_j)/2} \delta \right) \right\}. \tag{37}
\end{aligned}$$

This integral also has an odd term in δ , like $I_{ij, <r_{\pm}^2>}^{(0)}$. Its plot as a function of δ resembles that shown in Fig. 3C. That is, despite the $1/\delta$ factor in the last term, $I_{ij, <r_{\pm}>}^{(0)}$ is *not* singular at $\delta = 0$ (i.e., when there is no separation between the two wells): $I_{ij, <r_{\pm}>}^{(0)} \rightarrow 2/(\mu_i + \mu_j)^2$ as $\delta \rightarrow 0$.

The cross term for $\langle r_{\pm} \rangle$ is

$$\begin{aligned}
I_{ij, <r_{\pm}>}^{(1)} = & \frac{2}{(\mu_i + \mu_j)^2} \left(e^{-2\mu_i \delta^2} + e^{-2\mu_j \delta^2} - e^{-\frac{1}{2}(\mu_i + \mu_j) \delta^2} \right) \\
& + \frac{1}{2\delta \mu_i \mu_j} \left[\frac{\pi}{2(\mu_i + \mu_j)^5} \right]^{1/2} \left\{ (\mu_i + \mu_j)^2 \operatorname{Erfc} \left(\sqrt{\frac{\mu_i + \mu_j}{2}} \delta \right) \right. \\
& - 2 \mu_j (\mu_i + \mu_j + 4 \mu_i^2 \delta^2) e^{-\frac{2\delta^2 \mu_i \mu_j}{\mu_i + \mu_j}} \operatorname{Erfc} \left(\sqrt{\frac{2}{\mu_i + \mu_j}} \mu_i \delta \right) \\
& + 2 \mu_i (\mu_i + \mu_j + 4 \mu_j^2 \delta^2) e^{-\frac{2\delta^2 \mu_i \mu_j}{\mu_i + \mu_j}} \operatorname{Erf} \left(\sqrt{\frac{2}{\mu_i + \mu_j}} \mu_j \delta \right) \\
& \left. - (\mu_i - \mu_j) (\mu_i + \mu_j - 4 \mu_i \mu_j \delta^2) e^{-\frac{2\delta^2 \mu_i \mu_j}{\mu_i + \mu_j}} \operatorname{Erfc} \left(\frac{(\mu_i - \mu_j) \delta}{\sqrt{2(\mu_i + \mu_j)}} \right) \right\} \tag{38}
\end{aligned}$$

Note that $I_{ij, <r_{\pm}>}^{(1)}$ is also symmetric under the interchange of i and j and, again, at $\delta = 0$, we have $I_{ij, <r_{\pm}>}^{(1)} = 4/(\mu_i + \mu_j)^2 = 2 I_{ij, <r_{\pm}>}^{(0)}$. Its behavior as a function of δ is similar to that shown in Fig. 3D, again partly due to the presence of odd terms in δ .

VIII. THE OFF-DIAGONAL EXPECTATION OF $-i\alpha \cdot [(\nabla V(\mathbf{r})) + \beta(\nabla S(\mathbf{r}))]$

For the linear potentials of Eq. (7)

$$\nabla V(\mathbf{r}) = \nabla S(\mathbf{r}) = \begin{cases} \hat{\mathbf{r}}_- & \text{if } z > 0 \\ \hat{\mathbf{r}}_+ & \text{if } z < 0 \end{cases} \tag{39}$$

and we again have a simplification from the $(1 + \beta)$, namely,

$$-i\boldsymbol{\alpha} \cdot [(\nabla V(\mathbf{r})) + \beta (\nabla S(\mathbf{r}))] = -i\boldsymbol{\alpha} \cdot \hat{\mathbf{r}}_{\pm}(1 + \beta) = \begin{bmatrix} 0 & 0 \\ -2i \boldsymbol{\sigma} \cdot \hat{\mathbf{r}}_{\pm} & 0 \end{bmatrix}, \quad (40)$$

i.e., the operator \mathbf{X}_{12} in Eq. (15) vanishes and \mathbf{X}_{21} is doubled. The latter operator connects the upper component of Ψ^\dagger to the lower component of Ψ .

For the direct terms, Eq. (16) reduces to two terms

$$\begin{aligned} \langle [\nabla V S]^{(0)} \rangle &= -2 \frac{1}{4\pi} \sum_{i,j} \int d^3r \left\{ e^{-\mu_i r_-^2/2} [a_j b_i (\boldsymbol{\sigma} \cdot \mathbf{r}_-)(\boldsymbol{\sigma} \cdot \hat{\mathbf{r}}_{\pm})] e^{-\mu_j r_-^2/2} \right. \\ &\quad \left. + e^{-\mu_j r_-^2/2} [a_i b_j (\boldsymbol{\sigma} \cdot \mathbf{r}_-)(\boldsymbol{\sigma} \cdot \hat{\mathbf{r}}_{\pm})] e^{-\mu_i r_-^2/2} \right\} \\ &= \sum_{i,j} \left[a_j b_i K_{ij, <\nabla V S>}^{(0)} + a_i b_j K_{ji, <\nabla V S>}^{(0)} \right], \end{aligned} \quad (41)$$

where

$$K_{ij, <\nabla V S>}^{(0)} = -2 \frac{1}{4\pi} \int d^3r e^{-\mu_i r_-^2/2} [(\boldsymbol{\sigma} \cdot \mathbf{r}_-)(\boldsymbol{\sigma} \cdot \hat{\mathbf{r}}_{\pm})] e^{-\mu_j r_-^2/2}. \quad (42)$$

The Pauli matrices here reduce to [14]

$$(\boldsymbol{\sigma} \cdot \mathbf{r}_-)(\boldsymbol{\sigma} \cdot \hat{\mathbf{r}}_{\pm}) = r_- (\hat{\mathbf{r}}_- \cdot \hat{\mathbf{r}}_{\pm}). \quad (43)$$

For the integration over $z > 0$ the integrand becomes simply r_- , which is the same as that already needed for getting to the final result for $I_{<r_{\pm}>}^{(0)}$ in subsection VII B above. For the integration over negative z , however, Eq. (43) becomes

$$r_- (\hat{\mathbf{r}}_- \cdot \hat{\mathbf{r}}_+) = \mathbf{r}_- \cdot \mathbf{r}_+ / r_+ = (\rho^2 + z^2 - \delta^2) / \sqrt{\rho^2 + (z + \delta)^2}, \quad (44)$$

which involves a new integrand, but which nonetheless can still be done analytically. (Here it is much easier to do the ρ -integration first.) We find

$$\begin{aligned} K_{ij, <\nabla V S>}^{(0)} &= - \frac{2}{(\mu_i + \mu_j)^2} \left[2 - e^{-(\mu_i + \mu_j) \delta^2/2} \right] \\ &\quad - \frac{1}{\delta} \left[\frac{2\pi}{(\mu_i + \mu_j)^5} \right]^{1/2} \left[\text{Erf} \left(\sqrt{2(\mu_i + \mu_j)} \delta \right) - \text{Erf} \left(\sqrt{(\mu_i + \mu_j)/2} \delta \right) \right]. \end{aligned} \quad (45)$$

This result is, again, symmetric and non-singular with $K_{ij, <\nabla V S>}^{(0)} = -4/(\mu_i + \mu_j)^2$ at $\delta = 0$. In this case there are *no* odd terms (!) in δ . Its plot versus δ is similar to that shown in Fig. 3C, but with the initial slope at the origin being zero.

Because $K_{ij,<\nabla VS>}^{(0)} = K_{ji,<\nabla VS>}^{(0)}$, we can finally write the direct term contributions for this expectation as

$$< [\nabla VS]^{(0)} > = \sum_{i,j} (a_j b_i + a_i b_j) K_{ij,<\nabla VS>}^{(0)} , \quad (46)$$

regaining explicit symmetry.

The cross term integral $K_{<\nabla VS>}^{(1)}$ is more complicated but is done similarly. As $\mathbf{X}_{12} = 0$, there are now four terms remaining from Eq. (17),

$$\begin{aligned} < [\nabla VS]^{(1)} > = -2 \frac{1}{4\pi} \sum_{i,j} \int d^3 r \left\{ e^{-\mu_i r_+^2/2} [a_j b_i (\boldsymbol{\sigma} \cdot \mathbf{r}_+) (\boldsymbol{\sigma} \cdot \hat{\mathbf{r}}_{\pm})] e^{-\mu_j r_-^2/2} \right. \\ & \quad + e^{-\mu_i r_-^2/2} [a_j b_i (\boldsymbol{\sigma} \cdot \mathbf{r}_-) (\boldsymbol{\sigma} \cdot \hat{\mathbf{r}}_{\pm})] e^{-\mu_j r_+^2/2} \\ & \quad + e^{-\mu_j r_+^2/2} [a_i b_j (\boldsymbol{\sigma} \cdot \mathbf{r}_+) (\boldsymbol{\sigma} \cdot \hat{\mathbf{r}}_{\pm})] e^{-\mu_i r_-^2/2} \\ & \quad \left. + e^{-\mu_j r_-^2/2} [a_i b_j (\boldsymbol{\sigma} \cdot \mathbf{r}_-) (\boldsymbol{\sigma} \cdot \hat{\mathbf{r}}_{\pm})] e^{-\mu_i r_+^2/2} \right\} \\ & = \sum_{i,j} \int d^3 r [a_j b_i K_{ij,<\nabla VS>}^{(1)} + a_i b_j K_{ji,<\nabla VS>}^{(1)}] , \end{aligned} \quad (47)$$

where

$$\begin{aligned} K_{ij,<\nabla VS>}^{(1)} = -2 \frac{1}{4\pi} \int d^3 r \left\{ e^{-\mu_i r_+^2/2} [(\boldsymbol{\sigma} \cdot \mathbf{r}_+) (\boldsymbol{\sigma} \cdot \hat{\mathbf{r}}_{\pm})] e^{-\mu_j r_-^2/2} \right. \\ \left. + e^{-\mu_i r_-^2/2} [(\boldsymbol{\sigma} \cdot \mathbf{r}_-) (\boldsymbol{\sigma} \cdot \hat{\mathbf{r}}_{\pm})] e^{-\mu_j r_+^2/2} \right\} \end{aligned} \quad (48)$$

In addition to Eq. (43) we also need

$$(\boldsymbol{\sigma} \cdot \mathbf{r}_+) (\boldsymbol{\sigma} \cdot \hat{\mathbf{r}}_{\pm}) = r_+ (\hat{\mathbf{r}}_+ \cdot \hat{\mathbf{r}}_{\pm}) , \quad (49)$$

which becomes r_+ for the $z < 0$ integration and $(\rho^2 + z^2 - \delta^2)/\sqrt{\rho^2 + (z - \delta)^2}$ for the $z > 0$ integration.

The integrations over z go much easier if one re-defines the integrations over z in terms of $\mu = \mu_i + \mu_j$ and $\nu = \mu_i - \mu_j$. The resulting integrals in μ and ν can then be converted back to μ_i and μ_j . We find

$$\begin{aligned}
K_{ij, <\nabla VS>}^{(1)} = & \frac{1}{\mu_i \mu_j (\mu_i + \mu_j)^2} \left[2 \mu_j (\mu_j - \mu_i) e^{-2\mu_i \delta^2} + 2 \mu_i (\mu_i - \mu_j) e^{-2\mu_j \delta^2} \right. \\
& \left. - (\mu_i - \mu_j)^2 e^{-(\mu_i + \mu_j) \delta^2/2} \right] \\
& - \frac{1}{2 \delta \mu_i^2 \mu_j^2} \left[\frac{\pi}{2(\mu_i + \mu_j)^5} \right]^{1/2} \times \\
& \left\{ (\mu_i + \mu_j)^3 \left(\mu_i + \mu_j - 2\mu_i \mu_j \delta^2 \right) \operatorname{Erfc} \left(\sqrt{(\mu_i + \mu_j)/2} \delta \right) \right. \\
& + 2 \mu_i^2 \left[(\mu_i^2 + 4\mu_i \mu_j + 3\mu_j^2) - 4\mu_j^2 (\mu_i - \mu_j) \delta^2 \right] \\
& \quad \times e^{-2\mu_i \mu_j \delta^2/(\mu_i + \mu_j)} \operatorname{Erf} \left(\sqrt{2/(\mu_i + \mu_j)} \mu_j \delta \right) \\
& - 2 \mu_j^2 \left[3\mu_i^2 + 4\mu_i \mu_j + \mu_j^2 - 4\mu_i^2 (\mu_j - \mu_i) \delta^2 \right] \\
& \quad \times e^{-2\mu_i \mu_j \delta^2/(\mu_i + \mu_j)} \operatorname{Erfc} \left(\sqrt{2/(\mu_i + \mu_j)} \mu_i \delta \right) \\
& - \left[(\mu_i^3 + 5\mu_i^2 \mu_j + 5\mu_i \mu_j^2 + \mu_j^3) - 8\mu_i^2 \mu_j^2 \delta^2 \right] \\
& \quad \times (\mu_i - \mu_j) e^{-2\mu_i \mu_j \delta^2/(\mu_i + \mu_j)} \operatorname{Erfc} \left(\frac{(\mu_i - \mu_j) \delta}{\sqrt{2(\mu_i + \mu_j)}} \right) \left. \right\} , \tag{50}
\end{aligned}$$

which also is symmetric and goes to $-8/(\mu_i + \mu_j)^2 = 2 K_{ij, <\nabla VS>}^{(0)}$ at $\delta = 0$. This integral does have some odd terms in δ . Its plot as a function of δ resembles a Gaussian, i.e., looks like that shown in Fig. 3A.

Because $K_{ij, <\nabla VS>}^{(1)} = K_{ji, <\nabla VS>}^{(1)}$ we can again finally write

$$< [\nabla VS]^{(1)} > = \sum_{i,j} (a_j b_i + a_i b_j) K_{ij, <\nabla VS>}^{(1)} , \tag{51}$$

mirroring the form of Eq. (46).

IX. THE OFF-DIAGONAL EXPECTATION $-2i V(\mathbf{r}) \boldsymbol{\alpha} \cdot \nabla$

For this off-diagonal operator $\mathbf{X}_{12} = \mathbf{X}_{21} = -2V(\mathbf{r}) \nabla$ in Eq. (15) and the direct term expectation, Eq. (16), has all four terms

$$\begin{aligned}
< [2V\nabla]^{(0)} > = & \frac{1}{8\pi} \sum_{i,j} \int d^3r V(\mathbf{r}) \left\{ e^{-\mu_i r_-^2/2} \left[2 a_i b_j (\boldsymbol{\sigma} \cdot \nabla) (\boldsymbol{\sigma} \cdot \mathbf{r}_-) \right. \right. \\
& \quad \left. \left. - 2 b_i a_j (\boldsymbol{\sigma} \cdot \mathbf{r}_-) (\boldsymbol{\sigma} \cdot \nabla) \right] e^{-\mu_j r_-^2/2} \right. \\
& + e^{-\mu_j r_-^2/2} \left[2 a_j b_i (\boldsymbol{\sigma} \cdot \nabla) (\boldsymbol{\sigma} \cdot \mathbf{r}_-) \right. \\
& \quad \left. \left. - 2 b_j a_i (\boldsymbol{\sigma} \cdot \mathbf{r}_-) (\boldsymbol{\sigma} \cdot \nabla) \right] e^{-\mu_i r_-^2/2} \right\} . \tag{52}
\end{aligned}$$

With

$$\nabla_k e^{-\mu_i r_-^2/2} = -\mu_i(\mathbf{r}_-)_k e^{-\mu_i r_-^2/2}, \quad \nabla_k(\mathbf{r}_-)_l = \delta_{kl}, \quad \text{and} \quad (\boldsymbol{\sigma} \cdot \nabla)(\boldsymbol{\sigma} \cdot \mathbf{r}_-) = 3 \quad (53)$$

we have, for the first terms in the square brackets of Eq. (52),

$$\begin{aligned} (\boldsymbol{\sigma} \cdot \nabla)(\boldsymbol{\sigma} \cdot \mathbf{r}_-) e^{-\mu_i r_-^2/2} &= e^{-\mu_i r_-^2/2} (\boldsymbol{\sigma} \cdot \nabla)(\boldsymbol{\sigma} \cdot \mathbf{r}_-) + \boldsymbol{\sigma} \cdot [(\boldsymbol{\sigma} \cdot \mathbf{r}_-) \nabla e^{-\mu_i r_-^2/2}] \\ &= [3 - \mu_i(\boldsymbol{\sigma} \cdot \mathbf{r}_-)(\boldsymbol{\sigma} \cdot \mathbf{r}_-)] e^{-\mu_i r_-^2/2} = (3 - \mu_i r_-^2) e^{-\mu_i r_-^2/2} \end{aligned} \quad (54)$$

and similarly when acting on $e^{-\mu_j r_-^2/2}$.

For the second terms in the square brackets of Eq. (52),

$$(\boldsymbol{\sigma} \cdot \mathbf{r}_-)(\boldsymbol{\sigma} \cdot \nabla) e^{-\mu_i r_-^2/2} = -\mu_i(\boldsymbol{\sigma} \cdot \mathbf{r}_-)(\boldsymbol{\sigma} \cdot \mathbf{r}_-) e^{-\mu_i r_-^2/2} = -\mu_i r_-^2 e^{-\mu_i r_-^2/2} \quad (55)$$

and, again, similarly when acting on $e^{-\mu_j r_-^2/2}$.

With Eqs. (54) and (55), Eq. (52) reduces to

$$\begin{aligned} \langle [2V\nabla]^{(0)} \rangle &= \frac{1}{4\pi} \sum_{i,j} \int d^3r \left\{ e^{-\mu_i r_-^2/2} V(r_\pm) [a_i b_j (3 - \mu_j r_-^2) + b_i a_j \mu_j r_-^2] e^{-\mu_j r_-^2/2} \right. \\ &\quad \left. + e^{-\mu_j r_-^2/2} V(r_\pm) [a_j b_i (3 - \mu_i r_-^2) + b_j a_i \mu_i r_-^2] e^{-\mu_i r_-^2/2} \right\} \\ &= \sum_{i,j} \left\{ a_i b_j K_{ij, <2V\nabla>}^{(0)} + a_j b_i K_{ji, <2V\nabla>}^{(0)} \right\} \end{aligned} \quad (56)$$

where, with $V(r_\pm) = r_\pm - R$,

$$\begin{aligned} K_{ij, <2V\nabla>}^{(0)} &= \frac{1}{4\pi} \int d^3r e^{-\mu_i r_-^2/2} (r_\pm - R) [(\mu_i - \mu_j) r_-^2 - 3] e^{-\mu_j r_-^2/2} \\ &= (\mu_i - \mu_j) K_{ij, a}^{(0)} - (\mu_i - \mu_j) R K_{ij, b}^{(0)} + 3 K_{ij, c}^{(0)} - 3 R K_{ij, d}^{(0)} \end{aligned} \quad (57)$$

where these four integrals are

$$\begin{aligned} K_{ij, a}^{(0)} &= \frac{1}{4\pi} \int d^3r e^{-\mu_i r_-^2/2} r_\pm r_-^2 e^{-\mu_j r_-^2/2} \\ &= \frac{1}{2(\mu_j + \mu_i)^3} \left[16 + 6 e^{-2(\mu_j + \mu_i) \delta^2} - 11 e^{-(\mu_j + \mu_i) \delta^2/2} \right] \\ &\quad + \frac{1}{2\delta} \left[\frac{\pi}{2(\mu_j + \mu_i)^7} \right]^{1/2} \left\{ [5 + 9(\mu_j + \mu_i) \delta^2] \text{Erfc} \left(\sqrt{(\mu_j + \mu_i)/2} \delta \right) \right. \\ &\quad \left. - [5 + 12(\mu_j + \mu_i) \delta^2] \text{Erfc} \left(\sqrt{2(\mu_j + \mu_i)} \delta \right) \right\}, \end{aligned} \quad (58)$$

$$K_{ij, b}^{(0)} = \frac{1}{4\pi} \int d^3r e^{-\mu_i r_-^2/2} r_-^2 e^{-\mu_j r_-^2/2} = 3 \left[\frac{\pi}{2(\mu_j + \mu_i)^5} \right]^{1/2}, \quad (59)$$

$$K_{ij, c}^{(0)} = \frac{1}{4\pi} \int d^3r e^{-\mu_i r_-^2/2} r_\pm e^{-\mu_j r_-^2/2} = I_{ij, < r_\pm >}^{(0)}, \quad (60)$$

$$K_{ij, d}^{(0)} = \frac{1}{4\pi} \int d^3r e^{-\mu_i r_-^2/2} e^{-\mu_j r_-^2/2} = I_{ij, < 1 >}^{(0)}. \quad (61)$$

$K_{ij,a}^{(0)}$ has an odd term in δ and its plot resembles that shown in Fig. 3D. All four of the above integrals are symmetric in i and j , so we can finally write

$$< [2 V \nabla]^{(0)} > = \sum_{i,j} (a_j b_i + a_i b_j) K_{ij, <2 V \nabla>}^{(0)} = 2 \sum_{i,j} a_j b_i K_{ij, <2 V \nabla>}^{(0)}. \quad (62)$$

For the cross term, from Eqs. (54) and (55) and the like, Eq. (17) becomes

$$\begin{aligned} < [2 V \nabla]^{(1)} > &= \frac{1}{8\pi} \sum_{i,j} \int d^3 r V(r_{\pm}) \times \\ &\quad \left\{ e^{-\mu_i r_+^2/2} [2 a_i b_j (\boldsymbol{\sigma} \cdot \nabla)(\boldsymbol{\sigma} \cdot \mathbf{r}_-) - 2 b_i a_j (\boldsymbol{\sigma} \cdot \mathbf{r}_+)(\boldsymbol{\sigma} \cdot \nabla)] e^{-\mu_j r_-^2/2} \right. \\ &\quad + e^{-\mu_i r_-^2/2} [2 a_i b_j (\boldsymbol{\sigma} \cdot \nabla)(\boldsymbol{\sigma} \cdot \mathbf{r}_+) - 2 b_i a_j (\boldsymbol{\sigma} \cdot \mathbf{r}_-)(\boldsymbol{\sigma} \cdot \nabla)] e^{-\mu_j r_+^2/2} \\ &\quad + e^{-\mu_j r_+^2/2} [2 a_j b_i (\boldsymbol{\sigma} \cdot \nabla)(\boldsymbol{\sigma} \cdot \mathbf{r}_-) - 2 b_j a_i (\boldsymbol{\sigma} \cdot \mathbf{r}_+)(\boldsymbol{\sigma} \cdot \nabla)] e^{-\mu_i r_-^2/2} \\ &\quad \left. + e^{-\mu_j r_-^2/2} [2 a_j b_i (\boldsymbol{\sigma} \cdot \nabla)(\boldsymbol{\sigma} \cdot \mathbf{r}_+) - 2 b_j a_i (\boldsymbol{\sigma} \cdot \mathbf{r}_-)(\boldsymbol{\sigma} \cdot \nabla)] e^{-\mu_i r_+^2/2} \right\} \\ &= \frac{1}{4\pi} \sum_{i,j} \int d^3 r V(r_{\pm}) \left\{ e^{-\mu_i r_+^2/2} [a_i b_j (3 - \mu_j r_-^2) + b_i a_j \mu_j (\mathbf{r}_+ \cdot \mathbf{r}_-)] e^{-\mu_j r_-^2/2} \right. \\ &\quad + e^{-\mu_i r_-^2/2} [a_i b_j (3 - \mu_j r_+^2) + b_i a_j \mu_j (\mathbf{r}_+ \cdot \mathbf{r}_-)] e^{-\mu_j r_+^2/2} \\ &\quad + e^{-\mu_j r_+^2/2} [a_j b_i (3 - \mu_i r_-^2) + b_j a_i \mu_i (\mathbf{r}_+ \cdot \mathbf{r}_-)] e^{-\mu_i r_-^2/2} \\ &\quad \left. + e^{-\mu_j r_-^2/2} [a_j b_i (3 - \mu_i r_+^2) + b_j a_i \mu_i (\mathbf{r}_+ \cdot \mathbf{r}_-)] e^{-\mu_i r_+^2/2} \right\} \\ &= \sum_{i,j} \left\{ a_i b_j K_{ij, <2 V \nabla>}^{(1)} + a_j b_i K_{ji, <2 V \nabla>}^{(1)} \right\}, \quad (63) \end{aligned}$$

where

$$\begin{aligned} K_{ij, <2 V \nabla>}^{(1)} &= \frac{1}{4\pi} \int d^3 r (r_{\pm} - R) \left\{ e^{-\mu_i r_+^2/2} [(3 - \mu_j r_-^2) + \mu_i (\mathbf{r}_+ \cdot \mathbf{r}_-)] e^{-\mu_j r_-^2/2} \right. \\ &\quad \left. + e^{-\mu_i r_-^2/2} [(3 - \mu_j r_+^2) + \mu_i (\mathbf{r}_+ \cdot \mathbf{r}_-)] e^{-\mu_j r_+^2/2} \right\} \\ &= -\mu_j K_{ij,a}^{(1)} + \mu_j R K_{ij,b}^{(1)} + \mu_i K_{ij,c}^{(1)} - \mu_i R K_{ij,d}^{(1)} + 3 K_{ij,e}^{(1)} - 3 R K_{ij,f}^{(1)}. \quad (64) \end{aligned}$$

The first integral,

$$K_{ij,a}^{(1)} = \frac{1}{4\pi} \int d^3 r \left\{ e^{-\mu_i r_+^2/2} r_{\pm} r_-^2 e^{-\mu_j r_-^2/2} + e^{-\mu_i r_-^2/2} r_{\pm} r_+^2 e^{-\mu_j r_+^2/2} \right\}, \quad (65)$$

can be done using $\mu = \mu_i + \mu_j$ and $\nu = \mu_i - \mu_j$, noting that $\mu > |\nu|$. Writing

$$\begin{aligned} &e^{-\mu_i r_+^2/2} r_-^2 e^{-\mu_j r_-^2/2} + e^{-\mu_i r_-^2/2} r_+^2 e^{-\mu_j r_+^2/2} \\ &= 2 e^{-\mu(\rho^2 + z^2 + \delta^2)/2} \left\{ (\rho^2 + z^2 + \delta^2) \cosh(\nu \delta z) + (2z\delta) \sinh(\nu \delta z) \right\} \quad (66) \end{aligned}$$

displays the i, j symmetric and anti-symmetric parts explicitly. After converting back to μ_i and μ_j ,

$$\begin{aligned}
K_{ij,a}^{(1)} = & \frac{2}{\mu_j(\mu_i + \mu_j)^4} \left\{ [5\mu_j(\mu_i + \mu_j) + 4\mu_i^2\mu_j\delta^2] e^{-2\mu_i\delta^2} \right. \\
& + [(\mu_i + \mu_j)(-2\mu_i + 3\mu_j) + 4\mu_i^2\mu_j\delta^2] e^{-2\mu_j\delta^2} \\
& \left. + [(\mu_i + \mu_j)(\mu_i - 4\mu_j) - 4\mu_i^2\mu_j\delta^2] e^{-\frac{1}{2}(\mu_i + \mu_j)\delta^2} \right\} \\
& + \frac{1}{2\delta\mu_i\mu_j^2} \left[\frac{\pi}{2(\mu_i + \mu_j)^9} \right]^{1/2} \times \\
& \left\{ 2[\mu_i(\mu_i + \mu_j)^2(2\mu_i + 5\mu_j) + 4\mu_i\mu_j(\mu_i + \mu_j)(\mu_i^2 - 2\mu_i\mu_j + 3\mu_j^2)\delta^2 + 16\mu_i^3\mu_j^3\delta^4] \right. \\
& \quad \times e^{-2\mu_i\mu_j\delta^2/(\mu_i + \mu_j)} \operatorname{Erf}\left(\sqrt{2/(\mu_i + \mu_j)}\mu_j\delta\right) \\
& - 2\mu_j^2[3(\mu_i + \mu_j)^2 + 24\mu_i^2(\mu_i + \mu_j)\delta^2 + 16\mu_i^4\delta^4] \\
& \quad \times e^{-2\mu_i\mu_j\delta^2/(\mu_i + \mu_j)} \operatorname{Erfc}\left(\sqrt{2/(\mu_i + \mu_j)}\mu_i\delta\right) \\
& - [(\mu_i + \mu_j)^2(2\mu_i^2 + 5\mu_i\mu_j - 3\mu_j^2) + 4\mu_i\mu_j(\mu_i + \mu_j)(\mu_i^2 - 8\mu_i\mu_j + 3\mu_j^2)\delta^2 \\
& \quad - 16\mu_i^3\mu_j^2(\mu_i - \mu_j)\delta^4] e^{-2\mu_i\mu_j\delta^2/(\mu_i + \mu_j)} \operatorname{Erfc}\left(\frac{(\mu_i - \mu_j)}{\sqrt{2(\mu_i + \mu_j)}}\delta\right) \\
& \left. + (\mu_i + \mu_j)^3(2\mu_i + 3\mu_j) \operatorname{Erfc}\left(\sqrt{(\mu_i + \mu_j)/2}\delta\right) \right\}, \tag{67}
\end{aligned}$$

which is, as expected, not symmetric in i and j . It is, however, non-singular: $K_{ij,a}^{(1)} = 16/(\mu_i + \mu_j)^3$ at $\delta = 0$. Its plot resembles that in Fig. 3D.

The second integral is much simpler,

$$\begin{aligned}
K_{ij,b}^{(1)} = & \frac{1}{4\pi} \int d^3r \left\{ e^{-\mu_i r_+^2/2} r_-^2 e^{-\mu_j r_-^2/2} + e^{-\mu_i r_-^2/2} r_+^2 e^{-\mu_j r_+^2/2} \right\} \\
= & \left[\frac{2\pi}{(\mu_i + \mu_j)^7} \right]^{1/2} [3(\mu_i + \mu_j) + 4\mu_j^2\delta^2] e^{-2\mu_i\mu_j\delta^2/(\mu_i + \mu_j)}, \tag{68}
\end{aligned}$$

which is also non-symmetric, but only because of the term proportional to δ^2 . As a function of δ it looks like Fig. 3E.

Almost as complicated as $K_{ij,a}^{(1)}$, the third integral is

$$\begin{aligned}
K_{ij,c}^{(1)} &= \frac{1}{4\pi} \int d^3r \left\{ e^{-\mu_j r_+^2/2} r_{\pm} (\mathbf{r}_+ \cdot \mathbf{r}_-) e^{-\mu_i r_-^2/2} \right. \\
&\quad \left. + e^{-\mu_j r_-^2/2} r_{\pm} (\mathbf{r}_+ \cdot \mathbf{r}_-) e^{-\mu_i r_+^2/2} \right\} \\
&= \frac{1}{\mu_i \mu_j (\mu_i + \mu_j)^4} \left\{ 2\mu_j [(\mu_i + \mu_j)(4\mu_i - \mu_j) - 4\mu_i^2 \mu_j \delta^2] e^{-2\mu_i \delta^2} \right. \\
&\quad + 2\mu_i [(\mu_i + \mu_j)(4\mu_j - \mu_i) - 4\mu_i \mu_j^2 \delta^2] e^{-2\mu_j \delta^2} \\
&\quad \left. + [(\mu_i + \mu_j)(\mu_i^2 - 8\mu_i \mu_j + \mu_j^2) + 8\mu_i^2 \mu_j^2 \delta^2] e^{-\frac{1}{2}(\mu_i + \mu_j) \delta^2} \right\} \\
&\quad + \frac{1}{2\delta \mu_i^2 \mu_j^2} \left[\frac{\pi}{2(\mu_i + \mu_j)^9} \right]^{1/2} \times \\
&\quad \left\{ 2\mu_j^2 [(\mu_i + \mu_j)^2(4\mu_i + \mu_j) + 8\mu_i^2 (\mu_i + \mu_j)(2\mu_i - \mu_j) \delta^2 - 16\mu_i^4 \mu_j \delta^4] \right. \\
&\quad \times e^{-2\mu_i \mu_j \delta^2 / (\mu_i + \mu_j)} \operatorname{Erf} \left(\sqrt{\frac{2}{\mu_i + \mu_j}} \mu_i \delta \right) \\
&\quad - 2\mu_i^2 [(\mu_i + \mu_j)^2(4\mu_j + \mu_i) + 8\mu_j^2 (\mu_i + \mu_j)(2\mu_j - \mu_i) \delta^2 - 16\mu_i \mu_j^4 \delta^4] \\
&\quad \times e^{-2\mu_i \mu_j \delta^2 / (\mu_i + \mu_j)} \operatorname{Erfc} \left(\sqrt{\frac{2}{\mu_i + \mu_j}} \mu_j \delta \right) \\
&\quad + [(\mu_i + \mu_j)^2(\mu_i^2 + 5\mu_i \mu_j + \mu_j^2) - 24\mu_i^2 \mu_j^2 (\mu_i + \mu_j) \delta^2 + 16\mu_i^3 \mu_j^3 \delta^4] \\
&\quad \times (\mu_i - \mu_j) e^{-2\mu_i \mu_j \delta^2 / (\mu_i + \mu_j)} \left[1 + \operatorname{Erf} \left(\frac{(\mu_i - \mu_j)}{\sqrt{2}(\mu_i + \mu_j)} \delta \right) \right] \\
&\quad + (\mu_i + \mu_j)^3 [(\mu_i^2 + 3\mu_i \mu_j + \mu_j^2) - 2\mu_i \mu_j (\mu_i + \mu_j) \delta^2] \\
&\quad \left. \times \operatorname{Erfc} \left(\sqrt{(\mu_i + \mu_j)/2} \delta \right) \right\} ,
\end{aligned} \tag{69}$$

which is surprisingly both symmetric, $K_{ji,c}^{(1)} = K_{ij,c}^{(1)}$, and non-singular: $K_{ij,c}^{(1)} = 16/(\mu_i + \mu_j)^3$ at $\delta = 0$. This integral as a function of δ looks like Fig. 3B.

The fourth integral is also simple,

$$\begin{aligned}
K_{ij,d}^{(1)} &= \frac{1}{4\pi} \int d^3r \left\{ e^{-\mu_j r_+^2/2} (\mathbf{r}_+ \cdot \mathbf{r}_-) e^{-\mu_i r_-^2/2} + e^{-\mu_j r_-^2/2} (\mathbf{r}_+ \cdot \mathbf{r}_-) e^{-\mu_i r_+^2/2} \right\} \\
&= \left[\frac{2\pi}{(\mu_j + \mu_i)^7} \right]^{1/2} [3(\mu_j + \mu_i) - 4\mu_i \mu_j \delta^2] e^{-2\mu_i \mu_j \delta^2 / (\mu_i + \mu_j)} .
\end{aligned} \tag{70}$$

Its δ dependence, Fig. 3F, shows a relatively deeper minimum than that depicted in Fig. 3B. The fifth and sixth integrals are already familiar,

$$K_{ij,e}^{(1)} = \frac{1}{4\pi} \int d^3r \left\{ e^{-\mu_i r_+^2/2} r_{\pm} e^{-\mu_j r_-^2/2} + e^{-\mu_i r_-^2/2} r_{\pm} e^{-\mu_j r_+^2/2} \right\} = I_{ij,<r_{\pm}>}^{(1)} \tag{71}$$

$$K_{ij,f}^{(1)} = \frac{1}{4\pi} \int d^3r \left\{ e^{-\mu_i r_+^2/2} e^{-\mu_j r_-^2/2} + e^{-\mu_i r_-^2/2} e^{-\mu_j r_+^2/2} \right\} = I_{ij,<1>}^{(1)} . \tag{72}$$

These last three integrals, $K_{ij,d}^{(1)}$ through $K_{ij,f}^{(1)}$, are all symmetric in i and j .

X. PLOTTING H_D^2 TO FIND A MINIMUM ENERGY

We can now pull all these integrals together to get an analytic expression for $\langle H_D^2 \rangle$, from which we can look for a minimum squared energy. First, we define the (unnormalized) contribution, as a function of ϵ and δ , from the diagonal pieces,

$$\begin{aligned} H_{D,\text{diag}}^2(\epsilon, \delta) = \sum_{i,j} a_i a_j & \left[(1 + \epsilon^2) \left(I_{\langle \nabla^2 \rangle}^{(0)} + 4 I_{ij, \langle r_{\pm}^2 \rangle}^{(0)} - 4 R I_{ij, \langle r_{\pm} \rangle}^{(0)} + R^2 I_{ij, \langle 1 \rangle}^{(0)} \right) \right. \\ & \left. + \epsilon \left(I_{ij, \langle \nabla^2 \rangle}^{(1)} + 4 I_{ij, \langle r_{\pm}^2 \rangle}^{(1)} - 4 R I_{ij, \langle r_{\pm} \rangle}^{(1)} + R^2 I_{ij, \langle 1 \rangle}^{(1)} \right) \right] \\ & + \sum_{i,j} b_i b_j \left[(1 + \epsilon^2) \left(J_{ij, \langle \nabla^2 \rangle}^{(0)} + R^2 J_{ij, \langle 1 \rangle}^{(0)} \right) + \epsilon \left(J_{ij, \langle \nabla^2 \rangle}^{(1)} + R^2 J_{ij, \langle 1 \rangle}^{(1)} \right) \right]. \end{aligned} \quad (73)$$

Figure 6 displays a three-dimensional plot of $H_{D,\text{diag}}^2(\epsilon, \delta)/N^2(\epsilon, \delta)$. It shows a relatively shallow minimum at $\epsilon = 1$ and $\delta \approx 0.8$. Note the large value, a dimensionless squared-energy of ≈ 4 , which must be largely canceled by the off-diagonal contributions to achieve a squared-energy similar to that for the one-well case, $E^2 = 0.5685$.

The off-diagonal (unnormalized) contributions are

$$\begin{aligned} H_{D,\text{off-diag}}^2(\epsilon, \delta) = \sum_{i,j} a_i b_j & \left[(1 + \epsilon^2) \left(K_{ij, \langle \nabla V S \rangle}^{(0)} + K_{ij, \langle V \nabla \rangle}^{(0)} \right) \right. \\ & \left. + \epsilon \left(K_{ij, \langle \nabla V S \rangle}^{(1)} + K_{ij, \langle V \nabla \rangle}^{(1)} \right) \right]. \end{aligned} \quad (74)$$

Figure 7 gives the three-dimensional plot of $H_{D,\text{off-diag}}^2(\epsilon, \delta)/N^2(\epsilon, \delta)$. In contrast with $H_{D,\text{diag}}^2/N^2$, it has a repulsive hump around $\delta \approx 1$ as well as a shallow valley running from $\epsilon = 0$ to 1 for $\delta \approx 0.2$. In the final sum of diagonal and off-diagonal contributions that hump will fill in the minimum seen in Fig. 6.

Thus we finally combine the two contributions, defining a normalized

$$H_D^2(\epsilon, \delta) = \left[H_{D,\text{off-diag}}^2(\epsilon, \delta) + H_{D,\text{diag}}^2(\epsilon, \delta) \right] / N^2(\epsilon, \delta). \quad (75)$$

Figure 8 plots how H_D^2 , as a function of ϵ and δ , develops a long, flat valley for all values of ϵ at a separation of $\delta \approx 0.2$ (i.e., recalling the value of κ , a separation of ≈ 0.45 fm). Also important is the hump (reminiscent of a fission barrier) around $\delta \approx 0.9$ that will help to confine this four-quark system at $\delta \approx 0.2$. This hump corresponds to a repulsion between

two $Q - \bar{q}$ asymptotic meson states if the light quarks delocalize. There is very little, if any, barrier to coalescence at $\epsilon = 0$.

It is easier to see this behavior with a two-dimensional plot, Fig. 9, showing H_D^2 as a function of δ at $\epsilon = 1$, where the valley is deepest and the hump is highest.

The dimensionless squared-energy valley-depth at $\delta = 0.18$, $\Delta H_D^2 = 0.097$, corresponds to a binding energy of 155 MeV for this $bc\bar{u}\bar{d}$ four-quark mesonic state. The valley is surprisingly flat, as shown in Fig. 10, dropping only 0.0023 from $\epsilon = 0$ to $\epsilon = 1$, corresponding to an energy drop of about 24 MeV. This suggests that Zitterbewegung may play an important role in the nature of this meson.

XI. DISCUSSION

Figure 11 is a contour plot of the binding energy of the state in the ϵ - δ plane. It displays two remarkable features: The first is that, at very small ϵ , appropriate to the approach towards each other of the two asymptotic (B and D) mesons, there is no evidence of a repulsive barrier to the fusion of those mesons. The second is that the valley of attraction at small meson separation is very flat between small ϵ (~ 0.2) and $\epsilon = 1$. This indicates that there is little energy associated with fluctuations in the ϵ collective variable of the light quarks in the state. There may be a more significant amount associated with the δ collective variable, but this effect is suppressed by the large masses associated with the Born-Oppenheimer centers defined by the heavy quarks, at least when viewed non-relativistically as seems appropriate for them, due to their relatively large masses. We therefore expect little correction to our estimates of the mass of the four-quark state due to collective variable effects.

The dashed curve in Fig. 11 illustrates how two well-separated B and D mesons at $\epsilon = 0$ and large δ would come together to $\delta \approx 0.2$, corresponding to a heavy quark separation of ≈ 0.45 fm. This small separation makes it clear that long-range pion-exchange effects can be expected to be negligible. From $\epsilon \approx 0.2$, the four-quark state then slides down the nearly flat valley to $\epsilon = 1$ where it is most bound. Such a state is prevented from falling apart because of the “fission barrier” around $\delta \approx 0.9$.

We have ignored the possible color magnetic contributions from the interaction of the two light antiquarks, but this must be less than 50 MeV and we expect it to be even less

than half this value. This correction is not large compared to the extracted binding energy of order 150 MeV found in our calculations. Thus, by comparing our binding energy with the threshold for B and D mesons, we predict a (set of) states in the region of $7 \text{ GeV}/c^2$.

If our calculation may also be applied to a pair of c and \bar{c} quarks, there would be a four-quark bound state around $3.6 \text{ GeV}/c^2$. Although exotic, the recently discussed $X(3872)$ with $J^{PC} = 1^{++}$ [15] is too massive to correspond to any of the states implied here. However, if it included a strange quark instead one of the u or d quarks that we have explicitly considered, and we compare to the mass difference between the D and D_s mesons, it is conceivable that it would match with our calculations here. Moreover, as is well known from hadron spectroscopy and lattice studies, the light mass of the s quark does not seem to have a significantly different wave function or a different behavior from the lighter quarks, so a recalculation along the lines we have described here might well be relevant to this state. (Again, the issues of symmetrization vs. antisymmetrization would be completely obviated as all of the quarks would be distinguishable.)

Finally, we comment on the surprisingly small difference in binding energy between the “molecular” form of the bound state, ($\epsilon \approx 0.2$, as in nuclei [1]) and the four-quark limit ($\epsilon = 1$). If this feature is widespread in such heavy quark systems, it could go far towards explaining why it has been so difficult to identify unambiguous four-quark states.

XII. ACKNOWLEDGMENTS

This work was carried out in part under the auspices of the National Nuclear Security Administration of the U.S. Department of Energy at Los Alamos National Laboratory under Contract No. DE-AC52-06NA25396.

-
- [1] T. Goldman, K. R. Maltman, G. J. Stephenson, Jr., and K. E. Schmidt, Nucl. Phys. **A481**, 621 (1988).
 - [2] C. J. Benesh, T. Goldman, and G. J. Stephenson, Jr., Phys. Rev. C **48**, 1379 (1993) and Phys. Rev. C **68**, 045208 (2003).
 - [3] C. J. Benesh and T. Goldman, Phys. Rev. C **55**, 441 (1997)
 - [4] E.g., T. Goldman and R. R. Silbar, Phys. Rev. C **77**, 065203 (2008).

- [5] Fan Wang, Guang-han Wu, Li-jian Teng, and T. Goldman, Phys. Rev. Lett. **69**, 29012904 (1992).
- [6] P. R. Page, T. Goldman, and J. N. Ginocchio, Phys. Rev. Lett. **86**, 204 (2001).
- [7] T. Goldman and R. R. Silbar, Phys. Rev. C **85**, 015203 (2012).
- [8] N. Isgur and M. B. Wise, Phys. Lett. B **237**, 527 (1990), Phys. Rev. D **43**, 819 (1991), Phys. Rev. Lett. **66**, 1130 (1991), and Nucl. Phys. B **348**, 276 (1991).
- [9] See, e.g., M. Oka, Phys. Rev. D **31**, 2274 (1985), Phys. Rev. D **31**, 2773 (1985), and subsequent related articles.
- [10] J. Beringer et al. (Particle Data Group), Phys. Rev. D **86**, 010001 (2012). A convenient access to this data is to go on-line to <http://pdglive.lbl.gov/>.
- [11] In this paper we work as much as possible with dimensionless quantities with $\hbar = c = 1$. That is, δ , \mathbf{w} , \mathbf{r} , ρ , z , and R are dimensionless distances. The dimensionless potentials V and S in Eq. (4) are related to potentials \mathcal{V} and \mathcal{S} with dimension GeV by a factor of κ^2 , which has dimensions of GeV/fm. For example, \mathcal{S} could be denoted as $\mathcal{S}(\mathbf{r}) = \kappa^2 \mathbf{r}$, where $\mathbf{r} = \kappa \mathbf{r}$ has dimensions in fm. In GMSS [1], to cite one reference, κ^2 was chosen to be 0.9 GeV/fm, corresponding to $\kappa = 2.21 \text{ fm}^{-1}$. In this paper we have used a larger value, $\kappa^2 = 1.253 \text{ GeV/fm}$, or $\kappa = 2.520 \text{ fm}^{-1}$, as found in our fitting of charmonia masses.
- [12] R. R. Silbar and T. Goldman, Eur. J. Phys. **32**, 217 (2011).
- [13] M. Abramovitz and I. A. Stegun, *Handbook of Mathematical Functions*, (Dover, New York, 1965), Chap. 7.
- [14] Because we have separated the two wells along the z -direction, the cross product $\mathbf{r}_+ \times \mathbf{r}_-$ only has x and y components. Since we have assumed the Pauli spinor χ_{m_s} to be polarized along the z -axis, the term from the product of two Pauli σ matrices that gives a $i\boldsymbol{\sigma} \cdot \mathbf{r}_+ \times \mathbf{r}_-$ contribution vanishes.
- [15] LHCb collaboration 2013, LHCb-PAPER-2013001, to be submitted to Phys. Rev. Lett.

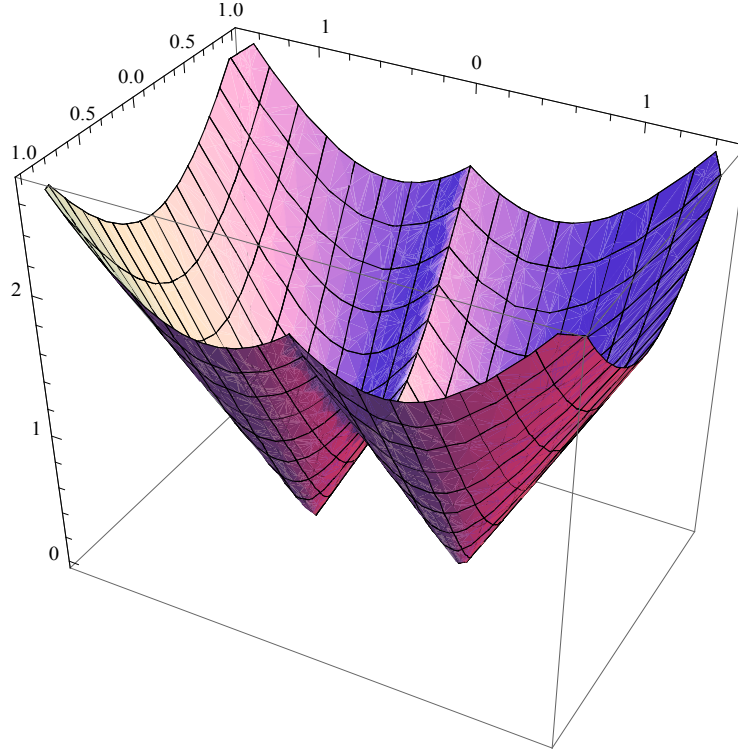


FIG. 1. Two-well linear potential.

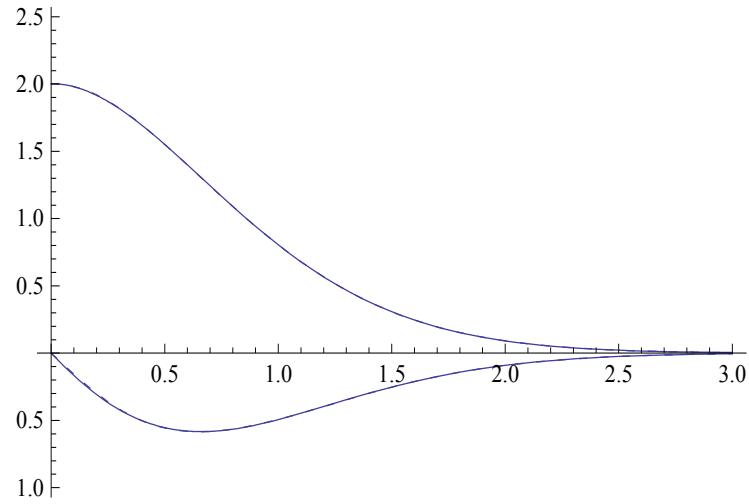


FIG. 2. Massless quark $1s$ wave functions $\psi_a(r)$ (above the axis) and $r\psi_b(r)$ (below).

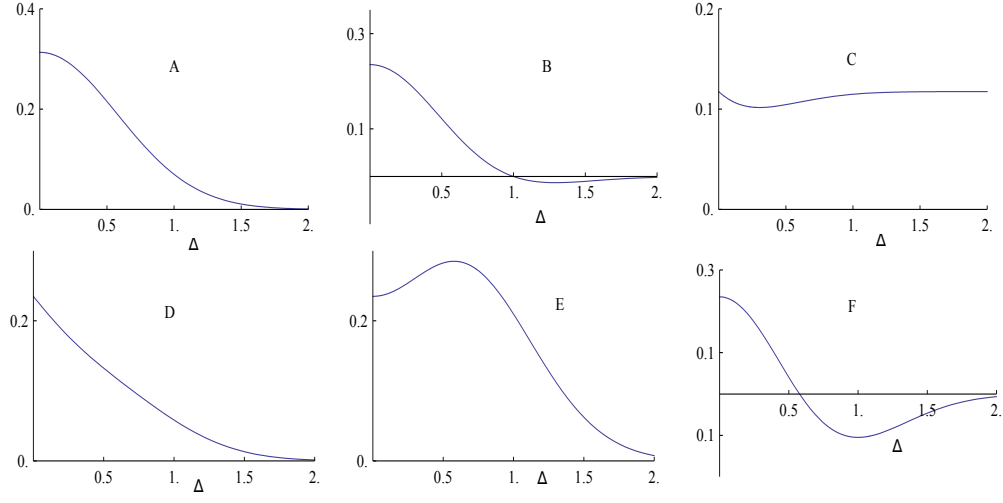


FIG. 3. Typical plots of I 's, J 's, and K 's as functions of δ .

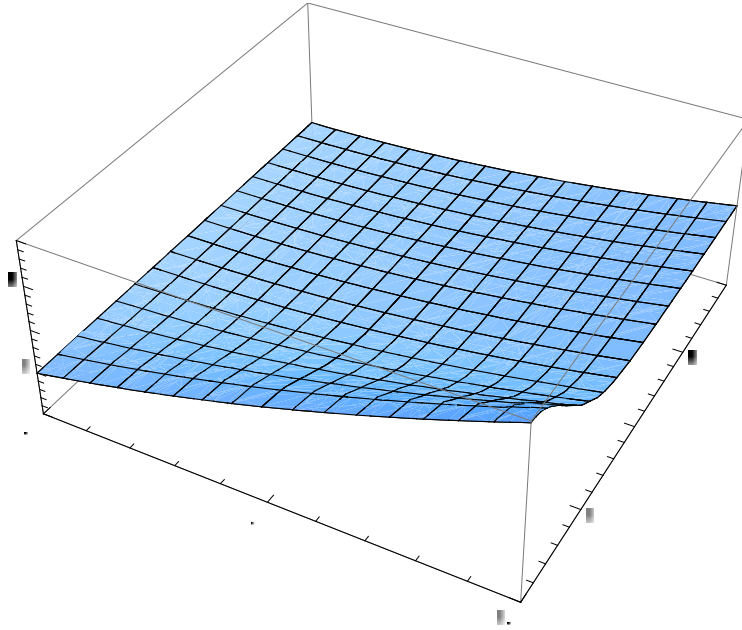


FIG. 4. Three-dimensional plot of $N^2(\epsilon, \delta)$.

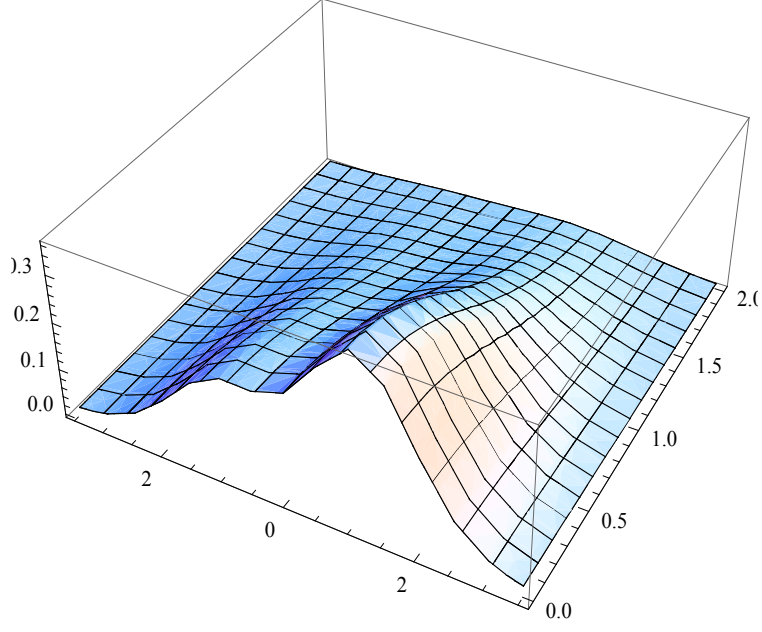


FIG. 5. Plot of $\Psi_a(\rho, z)$ for $\epsilon = 0.5$ and $\delta = 1.0$.

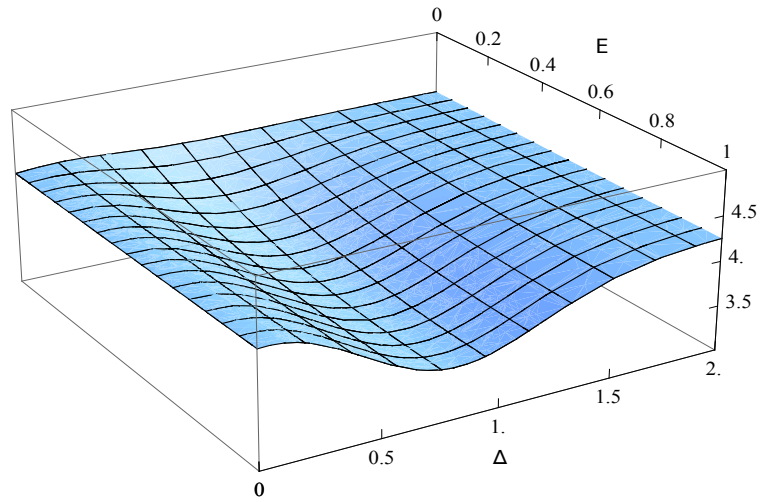


FIG. 6. Plot of the diagonal contribution to $H_D^2(\epsilon, \delta)$.

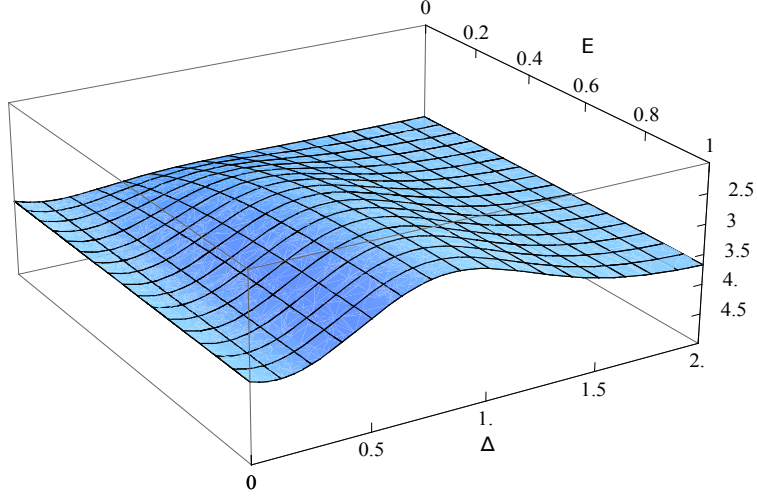


FIG. 7. Plot of the off-diagonal contribution to $H_D^2(\epsilon, \delta)$.

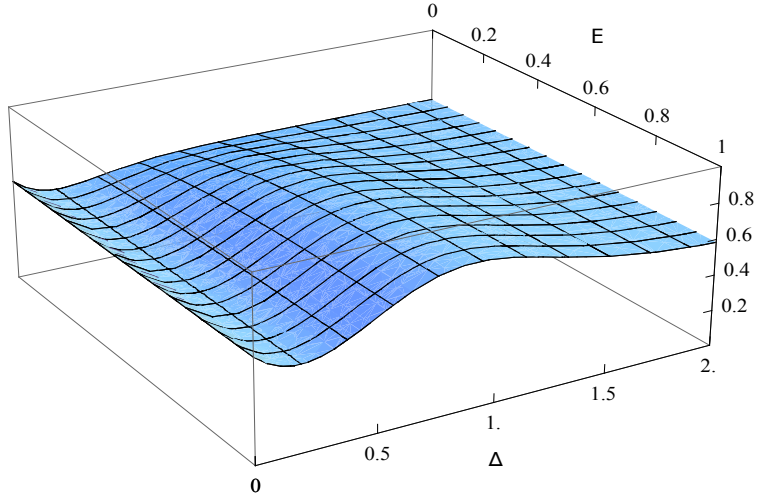


FIG. 8. Plot of the final $H_D^2(\epsilon, \delta)$.

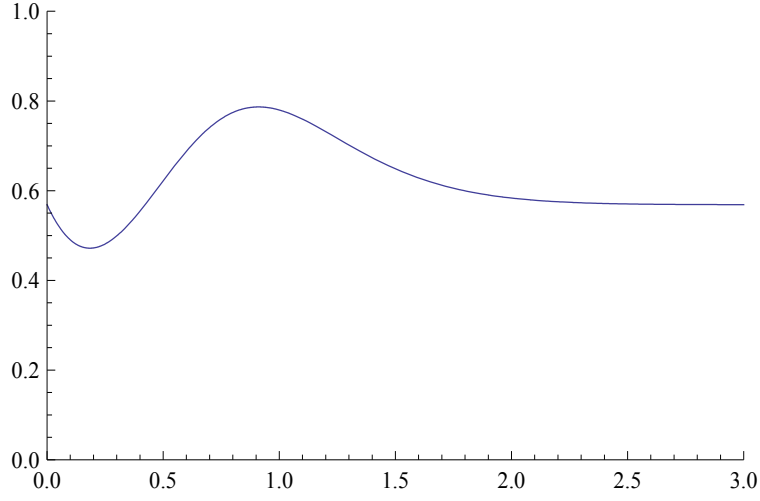


FIG. 9. Two-dimensional plot of $H_D^2(\epsilon = 1, \delta)$, showing the valley at $\delta = 0.18$ and the “fission barrier” at $\delta \approx 0.9$.

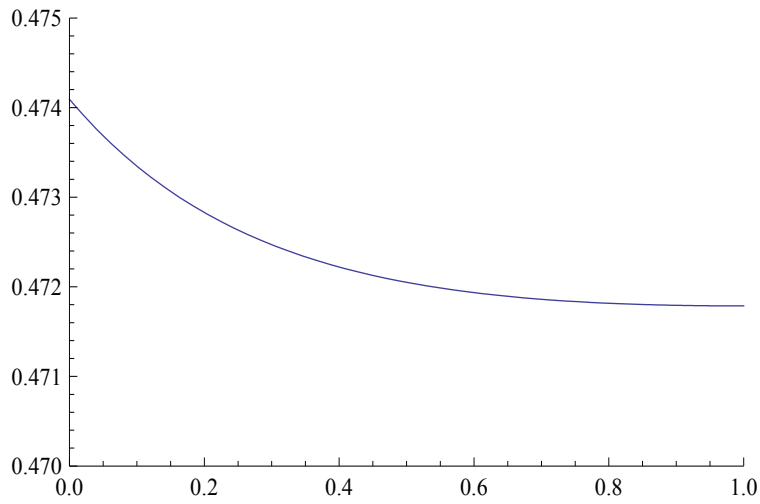


FIG. 10. Plot of how the nearly flat valley at $\delta = 0.18$ decreases from $\epsilon = 0$ to $\epsilon = 1$.

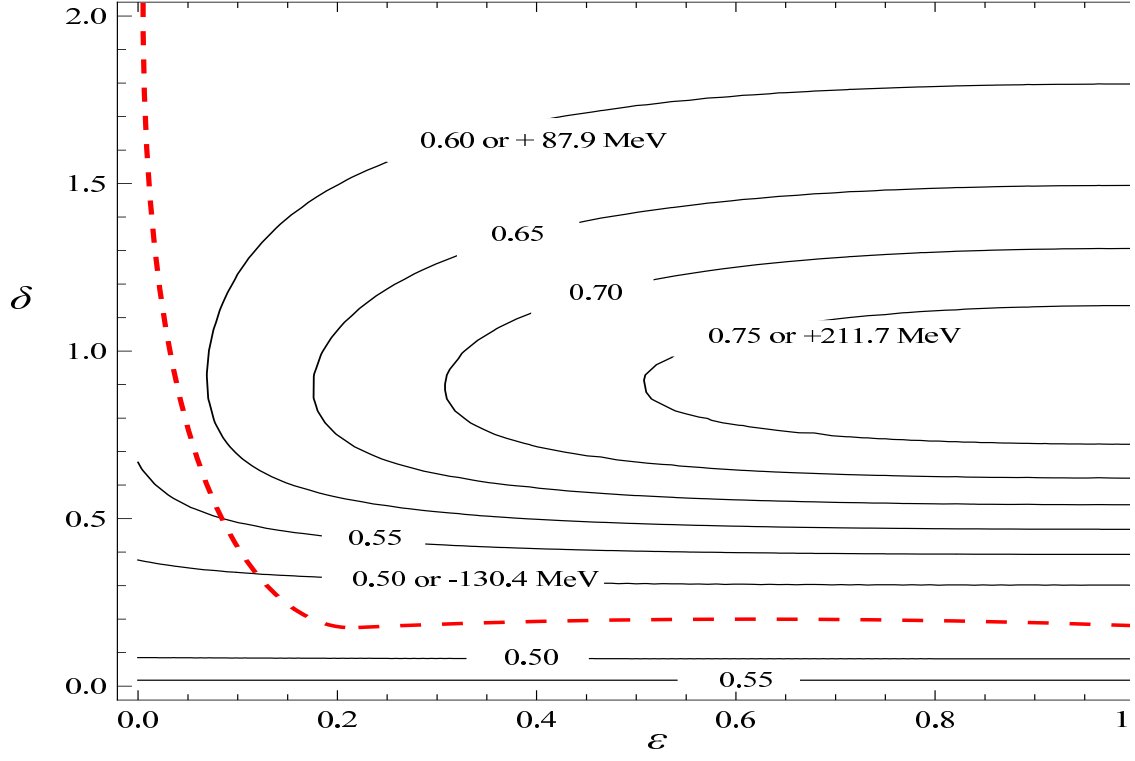


FIG. 11. Contour plot of $H_D^2(\epsilon, \delta)$. The dashed curve illustrates how two well-separated $Q - \bar{q}$ mesons at $\epsilon = 0$ and large δ would come together and slide down the valley at $\delta \approx 0.2$ to form a four-quark state at $\epsilon = 1$.